Manning, G. S. (1988) *Biopolymers 27*, 1529–1545.
Porschke, D., Zacharias, W., & Wells, R. D. (1987) *Biopolymers 26*, 1971–1974.
Rahmouni, A. R., & Wells, R. D. (1989) *Science 246*, 358–363.
Rice, J. A., & Crothers, D. M. (1989) *Biochemistry 28*, 4512–4516.
Sheardy, R. D. (1986) *Nucleic Acids Res. 16*, 1153–1167.
Sheardy, R. D., & Winkle, S. A. (1989) *Biochemistry 28*, 720–725.
Thomas, T. J. (1989) *Biophys. J. 55*, 240.
Thomas, T. J., & Bloomfield, V. A. (1983) *Nucleic Acids Res. 11*, 1919–1930.
Tung, C.-S., & Burks, C. (1987) *J. Biomol. Struct. Dyn. 4*, 553–559.
Wang, A. H.-J., Quigley, G. J., Kolpak, F. J., Crawford, J. L., van Boom, J. H., van der Marel, G., & Rich, A. (1979) *Nature 282*, 680–686.
Wu, H.-M., & Crothers, D. M. (1984) *Nature 308*, 509–513.
Zahn, K., & Blattner, F. R. (1985) *Nature 317*, 451–453.

NMR Studies of the Interaction of Chromomycin A_3 with Small DNA Duplexes. Binding to GC-Containing Sequences†

Debra L. Banville,‡ Max A. Keniry,‡,§ Michal Kam,‖ and Richard H. Shafer*,‡
Department of Pharmaceutical Chemistry, School of Pharmacy, University of California, San Francisco, California 94143, and Department of Organic Chemistry, The Weizmann Institute of Science, Rehovot 76100, Israel

Received July 19, 1989; Revised Manuscript Received December 4, 1989

ABSTRACT: The interaction of chromomycin A_3 with the oligodeoxyribonucleotides **1**, d(ATGCAT), **2**, d(ATCGAT), **3**, d(TATGCATA), and **4**, d(ATAGCTAT), has been investigated by ^1H and ^{31}P NMR. In the presence of Mg^{2+}, chromomycin binds strongly to the three GC-containing oligomers **1**, **3**, and **4** but not to the CG-containing oligomer **2**. The proton chemical shift changes for **1** and **3** are similar, and these DNA duplexes appear to bind with a stoichiometry of 2 drugs:1 Mg^{2+}:1 duplex. The same stoichiometry of 2 drugs:1 duplex is confirmed with **4**; however, proton chemical shift changes differ. An overall C_2 symmetry is exhibited by the drug complex with **1**, **3**, and **4**. At a molar ratio of 2.0 (drugs:duplex), no free DNA proton NMR signals remain. Two-dimensional nuclear Overhauser exchange spectroscopy (NOESY) of the saturated chromomycin complex with **1** and **3** positions both chromomycinone hydroxyls and the E carbohydrates in the minor groove and provides evidence suggesting that the B carbohydrates lie on the major-groove side. This is supported by several dipolar coupling cross-peaks between the drug and the DNA duplex. Drug-induced conformational changes in duplex **1** are evaluated over a range of NOESY mixing times and found to possess some characteristics of both B-DNA and A-DNA, where the minor groove is wider and shallower. A widening of the minor groove is essential for the DNA duplex to accommodate two drug molecules. This current minor-groove model is a substantial revision of our earlier major-groove model [Keniry, M. A., Brown, S. C., Berman, E., & Shafer, R. H. (1987) *Biochemistry 26*, 1058–1067] and is in agreement with the model recently proposed by Gao and Patel [Gao, X., & Patel, D. J. (1989a) *Biochemistry 28*, 751–762].

Chromomycin is an antitumor antibiotic belonging to the aureolic acid group (see Figure 1; Thiem & Meyers, 1979). Along with the related analogues mithramycin and olivomycin, chromomycin is believed to complex with double-stranded DNA, thereby inhibiting DNA and RNA synthesis (Remers, 1979; Miyamoto et al., 1979; Kersten & Kersten, 1974; Berlin et al., 1966; Wakisaka et al., 1963; Slavek & Carter, 1975; Gause, 1965; Ward et al., 1965; Behr et al., 1969; Hartmann et al., 1968). The mode of drug binding to DNA is essential in elucidating the potent antitumor behavior of the aureolic acid group of drugs. In the case of chromomycin, a large variety of techniques has been applied to achieve this goal (Van Dyke & Dervan, 1983; Fox & Howarth, 1985; Hayasaka & Inoue, 1969; Dagleish et al., 1974; Cobreros et al., 1982; Behr et al., 1969; Nayak et al., 1973; Ward et al., 1965).

Early spectrophotometric studies demonstrated that the anionic chromomycin binds to DNA only in the presence of dicationic metals, e.g., Mg^{2+} and Mn^{2+}. The apparent binding constant ($K_{app} \sim 10^5$–10^6 M^{-1}) is similar to that of the neutrally charged intercalator actinomycin (Kersten et al., 1966; Behr et al., 1969; Horwitz & McGuire, 1978). This comparison led some researchers to believe that the chromomycinone chromophore also intercalated into DNA (Behr et al., 1969; Horwitz & McGuire, 1978). In the first NMR studies of chromomycin binding to DNA we observed additional evidence in support of intercalation, based on ^{13}C and ^1H NMR experiments of calf thymus DNA and poly(dG-dC) (Berman & Shafer, 1983; Berman et al., 1988). However, subsequent high-resolution NMR analysis of the oligonucleotide complex with chromomycin demonstrated that binding occurred via a nonintercalative binding mode, despite the observation of chemical shift effects typical of intercalation (Berman et al., 1985; Keniry et al., 1987).

Footprinting studies demonstrated that the DNA binding site consists of three or more base pairs and usually contains two contiguous guanine–cytosine base pairs. Although the requirement for guanine or a 2-aminopurine substitute has been established for tight binding with the aureolic acids, evidence for olivomycin binding to poly(dA-dT)·poly(dA-dT) suggests that a weaker binding interaction ($K_{app} < 10^5$ M^{-1})

† Supported by USPHS Grant CA27343 awarded by the National Cancer Institute, DHHS.
‡ University of California.
§ Present address: Research School of Chemistry, Australia National University, Canberra, ACT 2601, Australia.
‖ The Weizmann Institute of Science.

0006-2960/90/0429-6521$02.50/0

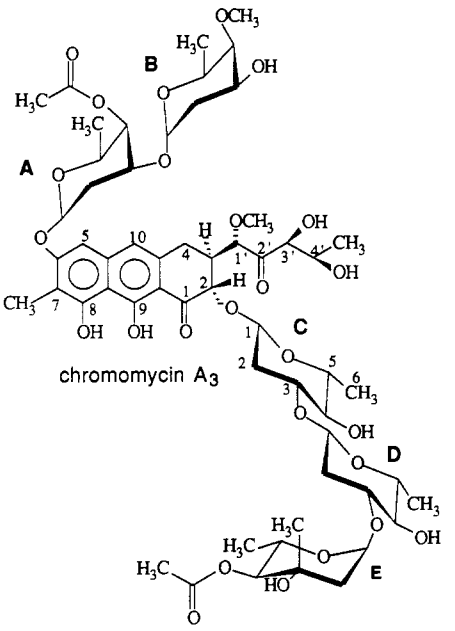

FIGURE 1: Structure of chromomycin A_3 as determined by the ^1H and ^{13}C NMR studies of Thiem and Meyer (1979).

is possible (Brikenshtein et al., 1983). Runs of AT base pairs, however, are not protected from enzymatic cleavage in footprinting studies (Van Dyke & Dervan, 1983; Fox & Howarth, 1985; Fox & Waring, 1986). Furthermore, these antibiotics do not inhibit RNA polymerase activity with the DNA templates poly(dA-dT)·poly(dA-dT), poly(dA)·poly(dT), and poly(dI)·poly(dC) (Ward et al., 1965). Thus, the presence of guanine is strongly implicated in the biological activity of the aureolic drug group but not required for the weaker binding mode seen with adenine–thymine base pairs.

Our recent two-dimensional ^1H NMR studies on the binding of chromomycin to the synthetic deoxyribonucleotide hexamer $d(ATGCAT)_2$, with excess Mg^{2+} present, resulted in the confirmation that chromomycin binds in a tightly bound nonintercalative drug–DNA complex (Keniry et al., 1987). These preliminary studies also suggested that the drug binds to the hexamer in 1 drug:1 duplex stoichiometry. Tentative nuclear Overhauser assignments placed the chromomycin AB carbohydrate chain and the chromophore near the major groove of the hexamer. This paper is a continuation of these NMR studies of chromomycin binding to the synthetic hexamer $d(ATGCAT)_2$. We present evidence that the stoichiometry of the saturated complex is 2 drugs:1 hexamer duplex:1 Mg^{2+} and that this 2:1:1 complex exhibits overall C_2 symmetry. The resulting conformational distortions of drug-bound $d(ATGCAT)_2$ are compared with the more general B- and A-DNA forms. We present evidence that places portions of chromomycin in the minor groove of $d(ATGCAT)_2$ and describe a general model to explain some of the proton–proton contacts obtained by NMR. This model represents a substantial revision from previously published results (Keniry et al., 1987) and is similar to that described by Gao and Patel (1989a,b) for the CRA–$d(TTGGCCAA)_2$ complex. Finally, questions of sequence selectivity are addressed by a comparative study of chromomycin binding to $d(ATCGAT)_2$, $d(TATGCATA)_2$, and $d(ATAGCTAT)_2$.

Materials and Methods

Chromomycin A_3 was purchased from Boehringer Mannheim Biochemica and used without further purification. The self-complementary oligonucleotide hexamers $d(ATGCAT)_2$ and $d(ATCGAT)_2$ and the octamer $d(TATGCATA)_2$ were purchased from Pharmacia and checked for purity by ^1H NMR and ^{31}P NMR. No further purification was necessary. The octamer $d(ATAGCTAT)_2$ was a gift from Dr. C. Levenson, Cetus Corp., and was purified by HPLC. For the Mg^{2+} titration, a stock magnesium chloride solution was obtained from Sigma and its concentration was verified independently by atomic absorption.

The NMR sample of $d(ATGCAT)_2$, 2 mM in duplex, was made by dissolving the hexamer in borate buffer (0.10 M borate, 0.18 M NaCl, and 0.015 M $MgCl_2$, pH 8.2) or phosphate buffer (20 mM sodium phosphate, 0.18 M NaCl, and 0.015 M Mg^{2+}, pH 8.2) as indicated and lyophilizing three times with D_2O (Aldrich, 99.96%). The $d(ATCGAT)_2$ and $d(ATAGCTAT)_2$ duplexes were prepared similarly in borate buffer and brought to final concentrations of 4 mM and 3 mM in duplex, respectively. A dilute stock solution of chromomycin A_3 was prepared by dissolving the solid in deionized water; undissolved drug was filtered out of the solution. Its concentration was determined by UV/visible spectroscopy with an extinction coefficient of 8800 M^{-1} cm^{-1} at 405 nm (Behr & Hartmann, 1965). The chromomycin titration was performed by lyophilizing aliquots of the drug several times with D_2O and then adding the hexamer solution to each aliquot in a glove bag under nitrogen to minimize the proton water signal. For the magnesium titration, the $d(TATGCATA)_2$ sample (2 mM in duplex) was prepared in borate buffer without $MgCl_2$ (2 mM borate and 0.10 M NaCl, pH 8.2). The final 0.4-mL sample contained 10% D_2O. Chromomycin was added as described above. Aliquots of Mg^{2+} were added from a concentrated solution of $MgCl_2$ in water.

The duplex concentrations were determined by UV spectroscopy. A small aliquot of duplex was added to a 0.1 M borate buffer solution, which also contained 1 M NaCl to maintain the integrity of the duplex at room temperature. The absorbance was measured at 260 nm, and estimated extinction coefficients of 79 200 [M (hexamer duplex)·cm]$^{-1}$ and 105 600 [M (octamer duplex)·cm]$^{-1}$ were used to determine molar concentrations. All ^1H spectra were collected on a General Electric GN-500 NMR spectrometer operating at a proton frequency of 500 MHz and processed on the Sun/AT&T system 4 computer using software developed at UCSF.

One-dimensional spectra of the low-field region (11–17 ppm) containing the imino protons of DNA and the phenolic proton of chromomycin were obtained with a $1\bar{3}3\bar{1}$ pulse sequence (Hore, 1983). NOE[1] data in the same region were obtained in the interleaved mode by taking the difference spectra from data sets with an on-resonance and off-resonance selective preirradiation pulse.

Two-dimensional phase-sensitive NOESY data (50-, 200-, and 400-ms mixing times) were acquired in the pure absorption mode by the method of States et al. (1982) with 4K data points in the t_2 dimension and 400 data points in the t_1 dimension. A minimum of 16 scans per t_1 increment was required for a sufficient signal-to-noise ratio and for utilizing the phase cycling routine. The bandwidth used was 5000 Hz, with a recycle delay of 5 s and a presaturation pulse on the residual HOD signal. In general, apodization was carried out the Gaussian window functions in the t_2 and t_1 dimensions. Prior to apodization each dimension was zero filled once to give final digital resolutions of 2.4 and 9.7 Hz/point along t_2 and t_1,

[1] Abbreviations: CRA, chromomycin A_3; NOE, nuclear Overhauser enhancement; NOESY, two-dimensional nuclear Overhauser exchange spectroscopy; HOHAHA, two-dimensional homonuclear Hartmann–Hahn relay spectroscopy; COSY, double-quantum-filtered correlation spectroscopy.

respectively. All proton chemical shifts were referenced to the HOD signal at 4.89 ppm.

Homonuclear correlation spectra (Aue et al., 1976; Neuhaus et al., 1985) were obtained with the double-quantum-filtered COSY experiment in the pure absorption mode and with the time-proportioned phase incrementation method (Redfield & Kuntz, 1975; Bodenhausen et al., 1980; Marion & Wuthrich, 1983). The data were collected with 2K data points in t_2 and 800 data points in t_1 and zero filled once in each dimension. A Gaussian window function was applied in both dimensions. A modified two-dimensional homonuclear Hartmann–Hahn relay experiment (HOHAHA; Hartmann & Hahn, 1962; Davis & Bax, 1985) was performed by using the MLEV-17 spin-lock pulse (Bax & Davis, 1985) with an Astron RS-4A amplifier and a 90° pulse of 37 μs. A total of 4K data points in t_2 and 400 data points in t_1 were collected, zero filled, and apodized by a Gaussian window function in both dimensions.

Proton-decoupled ^{31}P NMR spectra of d(ATGCAT)$_2$ were collected at 15 °C on the GN-500 spectrometer operating at the phosphorus frequency of 202 MHz. This one-pulse experiment used a 45° pulse (30 μs) and a 3-s repetition delay, with broad-band proton decoupling provided by a Waltz-64 decoupling pulse train (Shaka & Keeler, 1987). The ^{31}P NMR spectra of d(ATCGAT)$_2$ were collected at 97.5 MHz on a home-built wide-bore 5.6-T instrument equipped with a Nicolet 1180 data system and 292B pulse programmer (UCSF). All spectra were proton decoupled with a 2500-Hz sweep width, a 60° pulse (90° pulse widths were 45 μs), and a 2.8-s recycle time. Chemical shifts were referenced to an external capillary of 0.85% phosphoric acid.

Results

A series of one- and two-dimensional NMR experiments was carried out to study in detail the complex formed between chromomycin (CRA) and d(ATGCAT). A less detailed study with CRA was also carried out with d(ATCGAT), d(TATGCATA), and d(ATAGCTAT) for the purpose of qualitatively comparing these complexes with d(ATGCAT). For simplicity the DNA protons will be referred to by their position in the duplex starting from the 5′ end. For example, d(ATGCAT) is numbered A1-T2-G3-C4-A5-T6. The numbering scheme of Thiem and Meyer (1979) is used for chromomycin (see Figure 1). To avoid confusion between the drug and the DNA, the five CRA carbohydrates (A, B, C, D, and E) will only have a number designation for their protons. For example, 1A and 5C refer to the carbohydrate H1 and H5 protons of the A and C carbohydrates, respectively. Similarly, the chromomycinone and aliphatic side-chain protons will be distinguished from their carbohydrates by the Cr designation. For example, Cr5 and Cr1′ designate the chromophore H5 and aliphatic H1′ protons, respectively. Functional group proton designations are specified as Me (methyl), OMe (methoxy), and OAc (acetoxy). For example, the aliphatic side-chain methoxy proton on the 1′ carbon is referred to as Cr1′OMe.

NMR Study of CRA-d(ATGCAT)$_2$

One-Dimensional NMR Data of CRA-d(ATGCAT)$_2$. Formation of the chromomycin A$_3$–d(ATGCAT)$_2$ complex was followed by monitoring the imino proton region of the duplex. Prior to the addition of CRA, only the internal guanine and thymine imino protons (G3NH and T2NH) have well resolved signals (Figure 2A). As expected, due to fraying, the terminal thymine imino proton (T6NH) signal is exchange broadened and resonates farther upfield than the T2NH signal (Wuthrich, 1986; Chou et al., 1983; Ulrich et al., 1983).

Upon addition of CRA at a low ratio of drug:duplex concentrations, (R = 0.2), the T6NH signal appears to sharpen and shift downfield by 0.2 ppm and remains unshifted with the addition of more CRA. Thus, CRA has an immediate and significant stabilizing effect on the terminal base-pairing at a low R value. Unlike the T6NH behavior, the G3NH and T2NH signals are altered dramatically with each addition of CRA. The two new signals at 13.8 and 12.4 ppm were previously assigned to the drug-bound duplex protons T2NH and G3NH, respectively (Keniry et al., 1987). By a ratio of 1 drug:duplex (R = 1), the bound and free duplex signal areas are approximately equal in intensity.

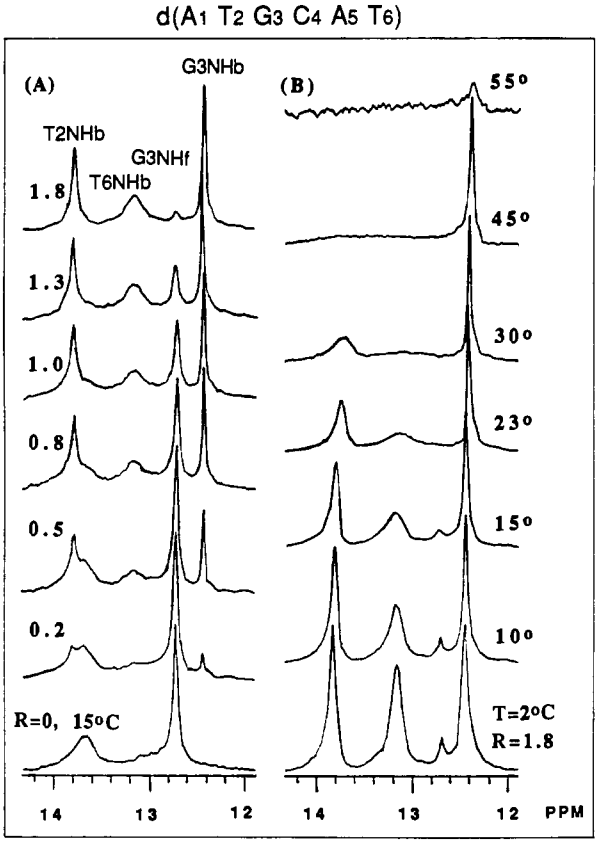

FIGURE 2: Imino proton region of the 2 mM duplex d(ATGCAT)$_2$ in a phosphate buffer containing excess $MgCl_2$ upon the addition of chromomycin A$_3$ (see Materials and Methods for details). (A) The molar ratios, R, of the chromomycin:duplex concentration range from 0 to 1.8 as indicated above. (B) The temperature for the R = 1.8 chromomycin–hexamer complex is raised from 2 to 55 °C.

At R = 2, the imino proton NMR spectrum is once again simplified to three signals where the original free duplex signals have been replaced by three new drug-bound duplex signals. Earlier work by Patel on the CRA complex with d(TTGGCCAA)$_2$ indicated a stoichiometry of 2 CRA:1 duplex (Patel, 1987). As can be seen in Figure 2, similar results are observed for the CRA complex with d(ATGCAT)$_2$. Saturation of d(ATGCAT)$_2$ occurs at R = 2 and not at R = 1 as implied earlier (Keniry et al., 1987). Furthermore, the simplicity of the imino proton region suggests that the 2:1 CRA–d(ATGCAT)$_2$ complex possesses C_2 symmetry. This is also consistent with the more recent results found for the CRA–d(TTGGCCAA)$_2$ complex (Gao & Patel, 1989a).

Evidence that CRA affects the stability of the double-stranded duplex can be observed in Figure 2. The relative full line widths at half-height for the two drug-bound imino proton signals at R = 1 are smaller than those for the two corresponding drug-free imino proton signals. The G3NH and T2NH line widths of 32 and 120 Hz are decreased to 20 and 40 Hz, respectively. A temperature-dependence study at R = 1.8 is displayed in Figure 2B. By 23 °C the original

Table I: Summary of ^{1}H Assignments of 2 mM d(ATGCAT)$_2$ in the Presence of 2 Chromomycin Molecules:DNA Duplex[a]

base (5′–3′)	H8,6	H5,2	H1′	H2′	H2′	H3′	H4′	H5′,5″	NH	NH_2
A1	8.38[b]	8.11[b]	6.22[b]	2.85	2.87[b]	4.87[b]	4.20[c]	3.92[c]		na[d]
	−0.20	−0.17	−0.01	0.00	−0.19	+0.01	+0.08	−0.11		
T2	7.63	1.42[b]	6.25	2.43[b]	2.87[c]	4.92	4.30[c]	na	13.77	
	−0.27	−0.04	−0.51	+0.03	−0.68	+0.01	−0.07		−0.12	
G3	7.62		5.97	2.57[e]	2.77[b]	4.40[c]	4.03[c]	na	12.41	7.58w[f]
	+0.31		−0.03	+0.16	−0.10	+0.62	+0.39		+0.31	5.72n
C4	7.14	5.24	5.53	1.82[c]	2.13[c]	4.27[2]	4.15[c]	na		8.32w
	+0.24	+0.18	+0.16	+0.59	−0.11	+0.60	+0.07			6.98n
A5	8.22	8.19[b]	6.78	2.83	2.83	4.93	4.84	na		na
	+0.12	−0.32	−0.46	+0.08	−0.07	+0.10	−0.41			
T6	7.44	1.43[b]	6.30	2.19	2.19	4.60	4.03[c]	na	13.14	
	−0.16	+0.10	−0.17	−0.24	−0.24	−0.04	+0.01		−0.1	

[a] The ^{1}H chemical shift data were collected at 15 °C in a borate buffer containing excess $MgCl_2$ and referenced to the HOD signal at 4.89 ppm. Chemical shift deviations of drug-free and drug-bound chemical shifts (i.e., shift of CRA-free hexamer − shift of CRA-bound hexamer, in ppm) were obtained for similar salt and temperature conditions and are included underneath each resonance assignment. [b] Chemical shift deviations ≥0.05 ppm between our earlier 4 mM duplex concentration study and our more recent 2 mM study. [c] New peak assignments. [d] na indicates that the peak is not assigned. [e] Reassigned peaks. [f] Watson–Crick amino protons (w) and non-Watson–Crick amino protons (n).

Table II: Summary of Chromomycin A_3 ^{1}H NMR Assignments in the Presence of d(ATGCAT)$_2$ Duplex (2:1 Complex)[a]

	sugar					aglycon			
position	A	B	C	D	E[b]				
1	5.73	5.25	4.82	(2.63)	5.43	Cr2	4.65[c]	Cr7	(2.85)
	−0.48	−0.17	+0.23	+1.98	−0.40		+0.08		
2e	2.55	1.87	(1.93)	2.53	2.42	Cr3	2.88	Cr1′	5.05[c]
	−0.46	−0.17	+0.56	−0.25	−0.42		−0.27		−0.36
2a	2.25	1.60	(1.74)	1.24	2.17	Cr4a	2.85	Cr1′f	3.45
	−0.10	+0.08	−0.06	+0.39	−0.16		+0.25		+0.05
3	4.43	4.17	2.28	3.82	1.60	Cr4e	2.65	Cr3′	4.27
	−0.44	−0.26	+1.32	−0.30	−0.24		+0.03		−0.04
4	5.36	3.56	3.03	3.05	5.17	Cr5	7.03	Cr4′	4.31
	−0.20	−0.37	+0.04	+0.03	−0.57		−0.37		+0.04
4F[d]	(1.67)	3.65			(2.28)	Cr10	6.68	Cr5′	1.37
	−0.27	−0.09					−0.01		−0.03
5	4.23	4.00	2.93	3.43	4.32	CrOH	16.02		
	−0.41	−0.13	+0.37	−0.05	−0.34		−0.27		
6	1.48	1.37	1.35	1.35	1.66				
	−0.24	−0.10	−0.02	0.00	−0.44				

[a] All chemical shifts are referenced to the HOD signal at 4.89 ppm (see text for details) and compared with the chemical shifts of chromomycin in CD_2Cl_2 at 30 °C (Kam et al., 1988); i.e., shift of free CRA in CD_2Cl_2 − shift of bound CRA in water is given in ppm. Parentheses indicate a tentative assignment. [b] New peak assignments. [c] Reassigned peaks. [d] Functional groups for A (acetoxy), B (methoxy), E (acetoxy), and the aglycon pentanyl side chain (methoxy).

drug-free G3NH signal has broadened into the base line. In contrast, the new drug-bound G3NH resonance still remains by 55 °C while its corresponding T2NH has disappeared by 45 °C. Hence, CRA stabilizes or protects the duplex from exchange with water and from thermal denaturation.

The ^{31}P NMR spectrum of d(ATGCAT)$_2$ has five signals due to the 5′ phosphates attached to five of the six bases (T2, G3, C4, A5, and T6). Two of these ^{31}P signals overlap at −1.0 ppm, while the other three are well resolved at −1.12, −1.21, and −1.28 ppm. Assignment of these hexamer phosphate signals was not attempted. Previous assignments made by Marion and Lancelot (1984) are not applicable since they were made under lower salt and higher temperature conditions, which resulted in large chemical shift differences from our spectra. The addition of CRA in the presence of Mg^{2+} at a ratio of 1 drug:1 duplex generates a more complex spectrum (supplementary Figure 1; Keniry et al., 1987). Three new resonances are resolved, one downfield resonance at −0.65 ppm and two new upfield resonances at −1.57 and −2.1 ppm. By a ratio of 2 drugs:1 duplex, the spectrum is once again simplified to five resonances: two overlapping resonances at about −2.06 and −2.12 ppm and three fully resolved resonances at −1.57, −1.22, and −0.65 ppm. The original resonances are no longer observed (supplementary Figure 1).

^{1}H Assignments of d(ATGCAT)$_2$ in the 2:1 Complex. Most of the uncomplexed DNA and complexed CRA–DNA resonances were assigned previously at $R = 1$ (Keniry et al., 1987). At $R = 2$, the complexed CRA–DNA assignments are essentially identical. Typical two-dimensional data at $R = 2$ are shown in Figures 3 and 4. To minimize line broadening, presumably from aggregation effects, the titration presented in this study was performed at a lower duplex concentration (2.0 or 1.5 mM in duplex) than the previous study (4 mM). Both this and the previous study show essentially the same results except for some residual line broadening at the higher (4 mM) concentration and small variations in the chemical shifts of the terminal protons. Analysis of the two-dimensional NMR data at $R = 2$ allowed confirmation of the previous assignments and additional deoxyribose assignments with a small correction for a few of these assignments. These changes and additions are noted in Tables I and II and are discussed below.

Sequential assignments of the duplex protons were made from NOESY, COSY, and HOHAHA data (Wuthrich, 1986, and references therein). The intranucleotide NOE contacts, H8 or H6 to H1′, and internucleotide contacts, H1′ to H8 or H6, traced out in Figure 3 at $R = 2$ are similar to our previous study at $R = 1$ but without the appearance of uncomplexed DNA proton signals. This sequential 5′ to 3′ walk is both complete and indicative of a singular C_2 symmetrical duplex. Also shown in Figure 3 are the adenine H2 cross-peaks, which will be described in further detail below.

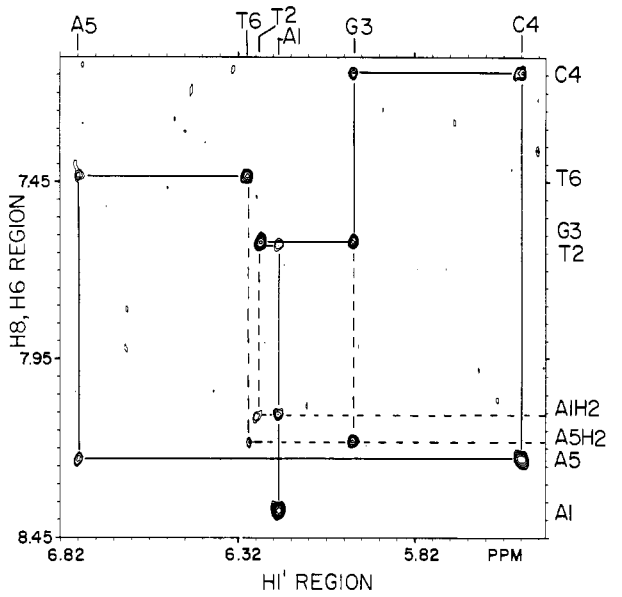

FIGURE 3: Expanded ^{1}H NOESY (200 ms) map of the aromatic base proton (H8, H6 and H2) to deoxyribose H1′ region at 15 °C. The complete NOE connectivities for the 2:1 complex of d(ATGCAT)$_2$ are traced out (solid line), and the connectivities to the two adenine H2 protons (AH2) are included (dotted line).

Assignment of all the H2′ and H2″ protons was accomplished by combining the COSY and HOHAHA data in the H1′ to H2′,H2″ regions. As shown in Figure 4, panels A and B, each H1′ resonance has two corresponding H2′,H2″ resonances for the G3, C4, and T2 nucleotides. A distinction can be made between the geminal H2′ and H2″ protons by comparing their NOE intensities with H1′ at short mixing times. This method does not require any assumptions about sugar pucker, since the proton–proton distance between H1′ and H2″ is always smaller than that between H1′ and H2′. For the uncomplexed hexamer, except in the case of overlap, the H2″ resonance is consistently downfield from that of H2′ (supplementary Figure 2). For the CRA–hexamer complex at R = 2, the H2″ resonance is consistently upfield from the H2′ resonance (Figure 4C). This chemical shift reversal is unusual for B-DNA helices (Jamin et al., 1985).

Assignments of the amino proton signals were possible with the R = 2 sample through analysis of the water NOESY spectrum (Wuthrich, 1986; Chou et al., 1983; Ulrich et al., 1983). Four amino proton signals are easily identified at 8.32, 7.58, 6.98, and 5.72 ppm. Strong NOE cross-peaks between the 8.32 and 6.98 ppm signals and between the 7.58 and 5.72 ppm signals suggest that each pair of resonances consists of the Watson–Crick and non-Watson–Crick protons, respectively (Figure 5). Resonances at 8.32 and 6.98 ppm are easily assigned to the amino protons of cytosine on the basis of their strong NOE cross-peaks with C4H5. Resonances at 7.58 and 5.72 ppm can be assigned to guanine on the basis of their 50-ms NOE contacts to G3NH (Figure 6B). A NOE contact between A5H2 and the non-Watson–Crick amino proton of guanine is expected and observed. Typically the amino protons of guanine are observed as a single resonance due to unhindered rotation about the carbon–nitrogen bond. But the presence of hydrogen bonding with one of the CRA protons or steric hindrance in the minor groove could hinder this rotation and lift the chemical shift degeneracy of the two guanine amino protons. The A5 and A1 amino proton resonances were not observed at 15 or 2 °C, and this is presumably due to base-catalyzed exchange with water (McConnell & Politowski, 1984, and references therein).

Of the four amino proton signals observed, only the signal assigned to the guanine Watson–Crick proton, the 7.58 ppm resonance, shows an apparent cross-peak to the water resonance at 4.89 ppm (Figure 5). Although the H3′ signals of A5, T2, and A1 also overlap with the H_2O signal, the G3 amino proton contact to these H3′ protons can be eliminated, since their distance is expected to be much more than 5 Å from G3NH$_2$ for either the B or A conformation of DNA. Hence, G3NH$_2$ is the only amino proton showing exchange with water on the NMR time scale.

Conformational Analysis of d(ATGCAT)$_2$ in the 2:1 Complex. Drug-induced distortions of d(ATGCAT)$_2$ away from the typical B-form can be assessed by a qualitative comparison of NOE data of the free and complexed oligonucleotide. The intranucleotide H8,H6/H2′ distance is smaller than the intranucleotide H8,H6/H3′ distance for B-DNA (C2′ endo sugar pucker), while the opposite holds for A-DNA (C3′ endo sugar pucker). In Table III, a comparison of these 50-ms NOESY intensities for the hexamer alone agree with the typical B conformation expected for this synthetic DNA. The intensities of the H8,H6/H2′ cross-peaks, particularly of the inner T2, G3, and C4 nucleotides, are 20–30 times more intense than those for the H8,H6/H3′ protons. Although chemical shift degeneracies for the 2:1 complex make this analysis incomplete, some unusual differences are noted between the free and bound oligonucleotide. For example, the C4H6 and A1H8 NOE contacts to their H3′ are observed, while their corresponding contacts to H2′ are not observed. Furthermore, the intensities of the H8,H6/H3′ contacts are

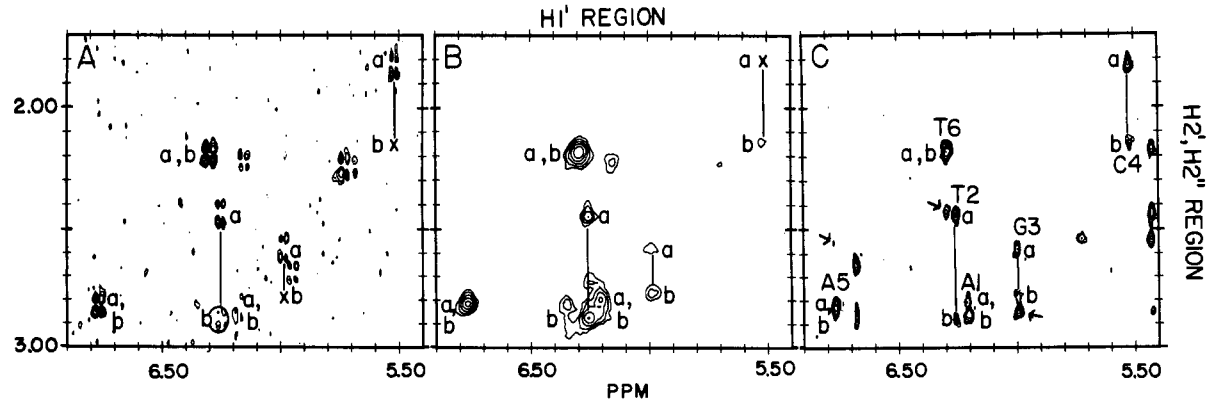

FIGURE 4: Three different two-dimensional NMR experiments with the 2:1 complex of CRA to d(ATGCAT)$_2$, demonstrating both the spin–spin coupling and the dipolar coupling between H1′ and the geminal protons H2′ and H2″. The double-quantum-filtered COSY and 70-ms HOHAHA experiments were carried out in phosphate buffer (A and B). The 50-ms NOESY was carried out in borate buffer (C). All three experiments were obtained at 15 °C.

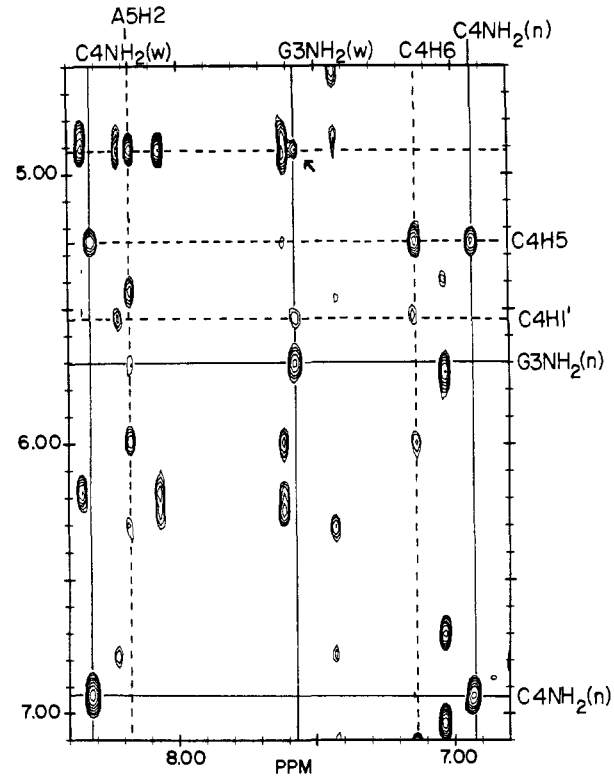

FIGURE 5: Water NOESY spectrum of the aromatic to deoxyribose H1′ region for a 2:1 CRA–d(ATGCAT)$_2$ complex in borate buffer containing 10% D_2O. The data were collected at 15 °C with a 290-ms mixing time. Four amino proton resonances are observed and assigned as labeled on the map. The solid line corresponds to labile resonances and the dotted line to nonlabile resonances. The arrow indicates a cross-peak between one of the GNH_2 resonances and the 4.89 ppm resonance.

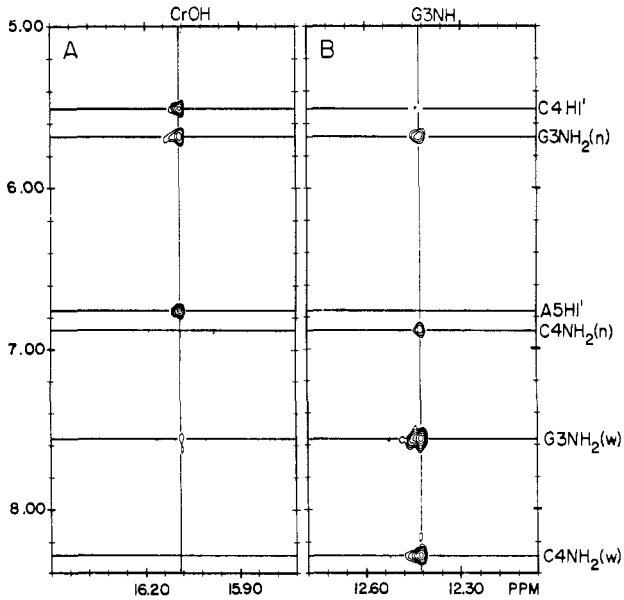

FIGURE 6: Spectrum from 50-ms NOESY, obtained in water (10% D_2O) with a selective excitation pulse, which shows both (A) strong chromomycin to DNA contacts from the ring hydroxyl to the typically minor-groove protons of d(ATGCAT)$_2$, as indicated, and (B) strong DNA to DNA contacts from the hydrogen-bonded G3NH to both of its nearly $G3NH_2$ and $C4NH_2$ protons. This experiment was obtained at 15 °C as described under Materials and Methods.

typically more intense for the complexed hexamer than for the uncomplexed hexamer, with one exception at the terminal nucleotide, T6. These differences may reflect changes in the average conformation of the deoxyribose ring pucker away from the usual C2′ endo conformation.

Table III: Selected List of 50-ms NOESY Cross-Peak Intensities between d(ATGCAT)$_2$ Alone and Its 2:1 Complex with Chromomycin[a]

(A) Intramolecular Cross-Peak Intensities						
cross-peak	A1	T2	G3	C4	A5	T6
H_2''–H_4'						
I_{free}	1.54	0.0	0.0	1.50	1.07	—
I_{bound}	—	5.57	8.22	0.0	—	—
$I_f - I_b$	—	−5.57	−7.22	+1.50	—	—
H8,6–H2′						
I_{free}	7.51	29.5	30.5	31.3	2.69	—
I_{bound}	0.0	—	—	0.0	—	—
$I_f - I_b$	+7.51	—	—	+31.3	—	—
H8,6–H2″						
I_{free}	1.09	4.48	6.18	4.18	3.34	—
I_{bound}	0.0	—	0.0	0.0	—	—
$I_f - I_b$	+1.09	—	+6.18	+4.18	—	—
H8,6–H3′						
I_{free}	0.0	1.18	1.51	1.29	0.56	4.81
I_{bound}	3.09	12.5	3.22	5.27	3.98	3.28
$I_f - I_b$	−3.09	−11.34	−1.71	−3.98	−3.42	+1.53

(B) Intermolecular Cross-Peak Intensities (from 5′ to 3′ End)					
cross-peak	A1–T2	T2–G3	G3–C4	C4–5A	A5–T6
H2′–H8,6					
I_{free}	0.90	4.68	—	2.54	4.99
I_{bound}	—	—	10.23	12.89	—
$I_f - I_b$	—	—	—	−10.35	—
H2″–H8,6					
I_{free}	7.41	8.19	8.53	4.96	11.40
I_{bound}	—	—	2.79	3.24	—
$I_f - I_b$	—	—	+5.74	+1.72	—
H3–H8,6					
I_{free}	0.00	0.00	1.05	0.56	0.96
I_{bound}	0.00	0.00	0.00	0.00	2.97
$I_f - I_b$	0.00	0.00	+1.05	+0.56	−2.01

[a] — indicates that the cross-peak overlapped with other resonances.

The average intranucleotide distance between H2″ and H4′ can also be used to compare the changes in ring pucker where this distance is typically much closer for A-DNA (2.4 Å) than for B-DNA (3.9 Å) (Wuthrich, 1986; Arnott & Hukins, 1972). The free hexamer has weak intensities for A1, C4, and A5 and no cross-peaks for T2 and G3 (Table III). In contrast, the T2 and G3 intensities for the 2:1 complex are observed and moderately strong, while the C4 cross-peak is not observed. These results together with the H8, H6 to H2′ and H3′ results strongly suggest a drug-induced distortion away from the usual C2′ endo sugar pucker of B-DNA. This distortion can be further confirmed by studying the COSY spin coupling patterns.

The vicinal coupling patterns for d(ATGCAT)$_2$ alone indicate a larger coupling between H1′/H2′ and H2′/H3′; however, the relative intensity of the H2″/H3′ cross-peak is too weak to observe in the COSY map (supplementary Figure 2A; Bax & Lerner, 1988). This pattern is consistent with a predominantly C2′ endo ring pucker. The vicinal coupling patterns for the 2:1 complex differ from those of the free hexamer. G3 and C4 have strong H1′/H2″ (Figure 4A) and H2″/H3′ COSY cross-peaks. Similarly, the T2 H1′/H2″ cross-peak is strong, but coupling from either of the geminal protons to H3′ is not observed. These results are consistent with the analysis of the NOESY cross-peak intensities discussed above that suggests a less B-like DNA conformation for the drug–DNA complex. Coupling between the H3′ and H4′ protons is generally observed in both the free and drug-bound duplex.

Strong sequential NOE contacts between the pyrimidine H5 proton and the H2′ and H2″ protons of the 5′-linked purine end are expected and observed, at a 50-ms mixing time, for the hexamer alone. Consistent with the B conformation, the

longer distance of the pyrimidine H5 to the 5′-linked purine H3′ precludes observation of these NOE contacts at the shorter mixing time for the free hexamer. In contrast, for the 2:1 complex, the internucleotide contacts from H5 to H2′ and H2″ are not observed at 50 ms for the C4–G3 and T6–A5 nucleotides but are observed for T2–A1. As in the uncomplexed hexamer, the A5H3′ to T6Me contact is not observed. Overlap of the G3H3′/C4H5 resonances with the CRA 1B/3A resonances prevents the assignment of this cross-peak. The A1H3′ resonance, however, does show a NOE contact to the neighboring T2Me. This is not observed for the uncomplexed DNA and is more consistent with a localized drug-induced distortion away from the B form of DNA. These data do not support an overall C3′ endo conformation, where the purine H3′ to pyrimidine H5 contact would be expected in all three instances at the shorter mixing time.

Intrastrand H8 to H6 contacts are longer range contacts for both the B (5.0 Å) and A (4.7 Å) conformations of DNA. For the hexamer alone, all five sequential base contacts are observed at the 200- and 400-ms mixing times. For the 2:1 complex, the G3H8/C4H6 and A1H8/T2H6 sequential base proton contacts are also observed at the longer mixing times, while the two base contacts between C4H6/A5H8 and A5H8/T6H6 are absent. The sequential purine H8 to pyrimidine H5 base contacts are shorter range (<4.0 Å) for both A and B forms of DNA. For the uncomplexed hexamer, all three of these contacts are observed at the 50-ms mixing time. For the 2:1 complex, the G3H8/C4H5 cross-peak is very weak at the 200-ms mixing time and not observed at the 50-ms condition. The lack of a G3H8/C4H5 contact at 50 ms is suggestive of a drug-induced disruption of the stacking at the guanine–cytosine base pairs.

In general, the AH2 is an isolated proton with only two direct dipolar contacts, the interstrand A1H2/A5H2 and A5H2/G3H1′ contacts (Wuthrich, 1986). While the A1H2/A5H2 NOE contact is observed at 200 ms for the free hexamer protons, its absence at $R = 1$ for the CRA-bound hexamer indicates a distortion in the helix. The A5H2/G3H1′ cross-peak is easily observed at the longer mixing times for both the drug-bound and drug-free hexamer protons. The relative weakness of the drug-free contact is consistent with a long cross-strand contact. But the stronger A5H2/G3H1′ contact in the bound oligonucleotide suggests a distortion that places these two protons closer together, as one would expect for a more A-like DNA conformation.

Various intrastrand, internucleotide contacts (A1H2 to T2H1′ and A5H2 to T6H1′, H2′, and H2″) as well as intranucleotide contacts (A1H2 to H1′) have been observed only at the longer mixing times for the complexed DNA. Contacts observed from AH2 to its own H1′ for the terminal adenine, but not the internal adenine, imply a greater conformational distortion at the terminal base pairs.

^{1}H NMR Assignments of Chromomycin A_3 in the 2:1 Complex. Assignments of bound drug protons for the 2:1 complex are summarized in Table II. The chemical shift assignments for the 2:1 complex and the 1:1 complex are essentially identical. Due to the simplification of the NOESY and COSY- data at $R = 2$ compared to $R = 1$, one correction in the $R = 1$ assignments was apparent. The aglycon proton chemical shifts of Cr2 and Cr1′ were switched and should be 4.65 and 5.05 ppm, respectively. These new data also made it possible to partially assign the C, D, and E sugar protons for the drug–DNA complex. The axial and equatorial protons located at the 2 position of each carbohydrate carbon have not been distinguished from each other. For convenience, the equatorial proton is assigned to the more downfield resonance from the axial proton.

The E sugar differs from the other four sugar groups in two important ways. The E sugar three-bond coupling is interrupted by the hydroxyl group at the 3E position, and it is the only sugar with two methyl groups (3MeE and 6MeE). The assignment strategy was to use these differences together with the previous E sugar assignments for CRA in nonaqueous solvents (Thiem & Meyer, 1979; Kam et al., 1988) as a guideline. Careful examination of the 200- and 400-ms NOESY data revealed two peaks in the methyl region at 1.60 and 1.66 ppm that have similar NOE contacts to other protons. Using the 1.66 ppm resonances as a starting point, it was possible to trace out the spin–spin coupling to a 4.32 ppm signal and then to a 5.17 ppm signal, whereupon the coupling ended. These three resonances were assigned to 6MeE, 5E, and 4E protons, respectively, and confirmed by their mutual NOEs. By the process of elimination, the 1.60 ppm resonance can then be assigned to the 3MeE protons. This assignment is confirmed in the 50-ms NOESY spectrum, where the 3MeE proton and 2aE and 2eE protons have strong NOE cross-peaks. These latter two resonances appear at 2.17 and 2.42 ppm and are assigned to the two 2E protons.

Assigment of the 1E proton was more difficult to make due to the absence of a COSY and NOESY cross-peak between the 1E and 2E protons. Instead, our 1E assignment at 5.43 ppm is based on the strong NOESY contacts from the 2E and 3MeE protons to this 5.43 ppm resonance and on comparison of these results with similar results found with a chromomycin analogue, mithramycin (unpublished results), where the 1E to 2E spin–spin coupling was resolved.

Definitive assignment of the uncoupled 4OMeE and Cr7 protons is not possible at this time. Both the 2.28 and 2.85 ppm resonances have strong NOE contacts with nearby E protons (2.28 to 2MeE and 6MeE and 2.85 to 1E, 4E, and 6E). The 2.28 ppm resonance has strong NOE contacts with the 3MeE and 6MeE. However, assignment of the 2.85 ppm resonance to Cr7 is also plausible. Intermolecular contacts between the E of one CRA and the Cr7 of the neighboring drug can occur while maintaining an overall 2-fold symmetry of the drug–DNA complex. On the basis of comparative results with mithramycin, this latter assignment is favored (unpublished results).

Additional assignments of the A and B sugar protons include both the axial and the equatorial protons at the 2A and 2B positions. These results were easily obtained by their mutual couplings in the COSY spectrum. COSY data at 15 °C, together with HOHAHA data at 25 °C, were sufficient to assign most of the C and D sugar protons (Table II). The COSY data suggest the possibility that the 3C resonance is dramatically shifted upfield to 2.28 ppm. Scalar coupling from 2.28 to 1.93 and 1.74 ppm signals and between 1.93 and 1.74 ppm signals suggests a tentative assignment of 2aC and 2eC to these two upfield resonances. The 1C resonance is assigned to 4.82 ppm on the basis of several NOESY contacts to 5C, 6C, and 2C. The 1D proton assignment is less clear; coupling from 2aD to 2eD and to the 2.63 ppm resonance implies that the 1D proton is at 2.63 ppm. Strong NOE contacts from this resonance to 5D and weaker contacts to 3D and 6D support this tentative assignment to 1D. This implies a relatively large chemical shift deviation of +1.98 ppm from that observed for CRA 1D in chloroform (Table II). Large upfield shifts can be attributed to ring current or charge effects or both.

The 90% water ^{1}H NMR spectrum of the 2:1 complex reveals one prominent hydroxyl signal at 16.02 ppm. A ten-

tative assignment of this downfield resonance is possible on the basis of the ^{1}H NMR spectrum of CRA alone. This resonance corresponds to the Cr9OH proton for CRA dissolved in dichloromethane (Thiem & Meyer, 1979), whereas the neighboring hydroxyl, Cr8OH, resonates farther upfield at 10 ppm. Since the relative pK_a's and chemical shifts of Cr9OH and Cr8OH could be altered in an aqueous environment with DNA and Mg^{2+}, we will simply refer to the 16.02 ppm resonance of the 2:1 complex as CrOH, a phenolic hydroxyl.

Conformational Analysis of the Drug Dimer. Analysis of the 50-ms NOESY spectrum is useful in observing NOE contacts due to direct dipolar coupling. More important, these proximate contacts can be used to build a three-dimensional model of the average drug conformation. Since CRA binds as a dimer, ambiguities involving intermolecular and intramolecular contacts are possible. The C_2 symmetry for the $R = 2$ complex can only occur by forming a 2-fold symmetrical drug dimer and by placing it about the helical axis of 2-fold symmetry. On the basis of this symmetry and the size of the drug and the DNA binding site (about three base pairs), intermolecular drug–drug contacts are highly probable.

Intramolecular Drug Contacts. Placement of the AB sugar chain with respect to the aglycon ring system hydrocarbon side chain is possible by examining the 50-ms NOESY data. As mentioned in our earlier study, a very strong 1A and a weaker 5A to Cr5 proton cross-peak point the A sugar away from the Cr7 methyl proton and place the 1A and 5A protons within 4 Å of the Cr5 proton (Keniry et al., 1987). Strong A and B proton cross-peaks suggest that the 1B proton points toward the 4A and 3A protons. Hence, the relative positions of the A and B rings are such that their H1 protons both point roughly in the same direction. No A or B proton contacts with the aliphatic side chain are observed. The lack of contacts between B and the chromophore suggests that this carbohydrate is more than 4 Å from the chromophore protons (Cr5, Cr10, Cr4a, and Cr4e).

The Cr1′OMe protons on the aliphatic side chain have a strong 50-ms NOE cross-peak with Cr1′ of its own side chain plus a slightly weaker contact to Cr4′. There are no detectable 50-ms NOE contacts between these aliphatic protons and the chromophore. At longer mixing times, some of these contacts are observed (from Cr10 to Cr1′OMe, Cr1′, and Cr4′ and from Cr3,4a to Cr1′OMe). Therefore, the aliphatic side chain is in the vicinity of the chromophore but not necessarily within 4 Å of its nearest chromophore protons.

No C to D proton contact is observed at the 50-ms NOESY mixing time, which suggests that the C and D carbohydrates are directed away from each other. However, 200-ms NOE contacts from 1D to 3C and 4D are observed. The D and E carbohydrates show several 50-ms NOE contacts from 1E to 2aD, 2eD, and 3D and from 3MeE to 4D, which places the D and E carbohydrates in much closer contact with each other than with the C carbohydrate.

Contacts between the aliphatic side chain and the C carbohydrate are observed. Cr1′OMe NOE contacts to 5C place this side chain near the C carbohydrate of its own drug. In consideration of this 5C contact, another Cr1′OMe contact to the ambiguous 6C, 6D resonance may be assigned to the 6C proton. Longer 200- and 400-ms mixing time contacts arise from Cr1′OMe to the chromophore (Cr2, Cr10, Cr3 or 4a, and Cr4e), to the C carbohydrate (3C or 4C) protons, and to an unassigned resonance at 4.09 ppm.

Intermolecular Drug Contacts. Several 50-ms NOE contacts from 5D to the AB chain (1A, 4B, 4OMeB) and chromophore (Cr5, Cr4e) are observed. These chromophore assignments are supported by 200-ms NOESY contacts from 3D to Cr5 and Cr4e. Contacts from 5D to the tentatively assigned 4OAcA resonance at 1.67 ppm are also observed. The latter resonance is near the 6MeE resonance at 1.66 ppm but clearly differs from 6MeE in the 25 °C 200-ms NOESY experiment. The 6MeD protons also show 50-ms NOE contacts to Cr4e and the 1.67 ppm resonance. The presence of these cross-peaks suggests the possibility that there is an intermolecular contact with 4OAcA. At longer mixing times the Cr10 and Cr3, 4a contacts to the 5D proton are observed, and the 6MeD, 6MeC protons have contacts to the A carbohydrate (1A and 4A) as well as the chromophore (Cr5, Cr10, Cr2). Although the 6MeD and 6MeC methyl proton chemical shifts are identical, the presence of many 5D contacts suggests that the other complementary drug–drug contacts are due to 6MeD and not 6MeC.

Conformational Analysis of the DNA–Drug Complex. The extensive overlap of drug and DNA proton resonances, the presence of two drugs, and the possibility of small local deviations from C_2 symmetry plus several unidentified resonances complicate the task of sorting through potential drug–DNA NOE contacts. Nevertheless, several well-defined NOE contacts between CRA and d(ATGCAT)$_2$ are identified and classified as strong or weak contacts, on the basis of the cross-peak intensities as a function of mixing time.

Strong Drug–DNA NOE Contacts. The distinct chemical shift of the CRA phenolic hydroxyl, CrOH, allows a unique probe of the chromophore position with respect to the DNA. In Figure 6, the 90% water NOESY map at the 50-ms mixing time shows two strong contacts from CrOH to the nonlabile A5H1′ and C4H1′. This places the hydrophilic edge of the chromophore into the minor groove of DNA. At 50 ms, CrOH contacts to both of the minor-groove amino protons of G3 are observed, where the exposed, non-Watson–Crick cross-peak is more intense than the hydrogen-bonded cross-peak. Contacts from CrOH to the G3 imino protons are only observed at the longer mixing time of 290 ms. Only one very weak contact from CrOH to the nonexchangeable proton A5H8 is observed at this longer mixing time. This is consistent with a long-range NOE contact to the major groove. Furthermore, the major-groove C4NH$_2$ amino protons do not show NOE contacts to CRA at either mixing time. These data are consistent with placement of the chromophore in the minor groove.

The strongest of the nonlabile proton contacts involve the E carbohydrate and the minor-groove side protons of DNA: 1E to A5H2 and T6H1′, and 4E to T2H1′ are observed at all three mixing times (see Figure 7). These contacts are supported by the existence of 200-ms NOESY cross-peaks from 6MeE to T2H1′ and A5H2 and from 2eE to A5H2. These contacts firmly place the E carbohydrate in the minor groove of d(ATGCAT)$_2$.

Weak Drug–DNA NOE Contacts. Similar to 6MeE, 5D (3.43 ppm) shows a 200-ms NOE contact to G3H1′. This contact, however, is not observed at 50 ms and is very weak at the longer mixing times. Strong coupling from the 3.43 ppm resonance to the 3.54 ppm resonance is observed in the COSY data. Thus, the 3.43 ppm resonance is shared by two coupled resonances, 5D and a currently unassigned resonance. One possible assignment for this proton resonance would be the DNA G3H5′ or G3H5″ protons. The lack of observable H4′ to H5′ or H5″ coupling precludes confirmation of this assignment.

Evidence for B carbohydrate contacts with DNA is present in the 200- and 400-ms NOESY data (Figure 8). At 400 ms, the T2H6, G3H8 peak has contacts to three B carbohy-

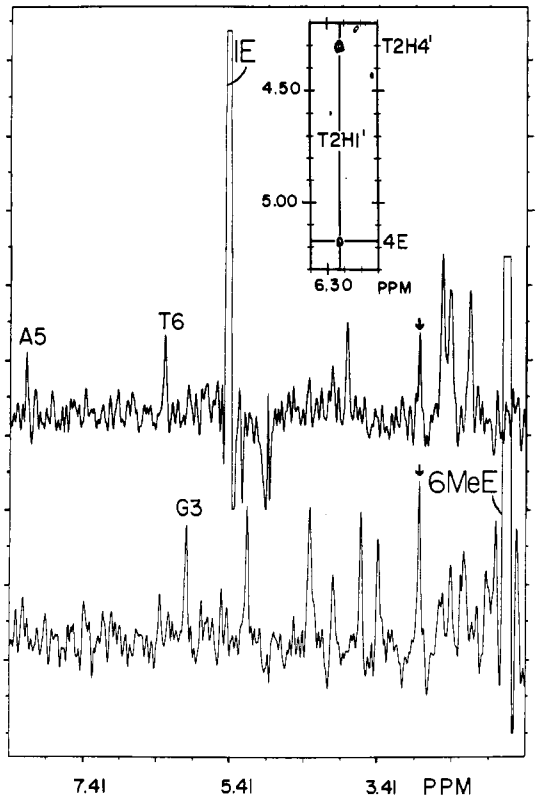

FIGURE 7: Data from 50-ms NOESY at 15 °C, shown to emphasize the closeness of these drug–DNA protons. Contacts from the 1E proton at 5.43 ppm to the 2eE, 2aE, 2eD, and 3D protons (upper slice) can be compared with strong contacts to A5H2, T6H1′, and an unidentified resonance at 2.85 ppm as indicated by an arrow. The drug–DNA contacts are supported by contacts from 6MeE to G3H1′ (lower slice) and from 4E to T2H1′ (inset).

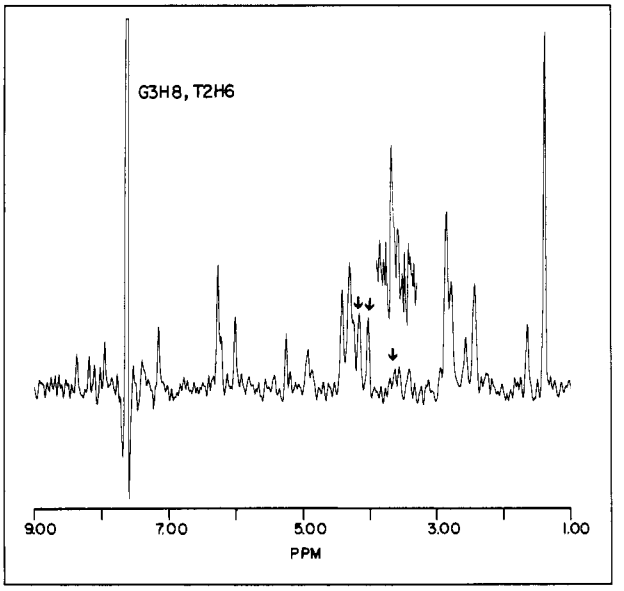

FIGURE 8: Evidence for NOE contacts between CRA and the major-groove proton G3H8 or T2H6 at the longer 400-ms mixing time. The t_1 increment show two strong NOE contacts from T2H6, G3H8 (7.76 ppm) to 3B and 5B as indicated by the left and middle arrows, respectively. A contact to 4OMeB (right arrow) is very weak at this 2 mM duplex concentration but clearly observed at 4 mM, as shown in the overlay above. Both experiments were carried out at 15 °C.

drate proton resonances (3B, 5B, and 4OMeB) at the 4 mM duplex concentration. At the lower 2 mM duplex concentration, the 4OMeB contact is significantly weaker. In conclusion, the coincidence of three potential CRA B to DNA G3H8, T2H6 contacts supports the placement of B near these

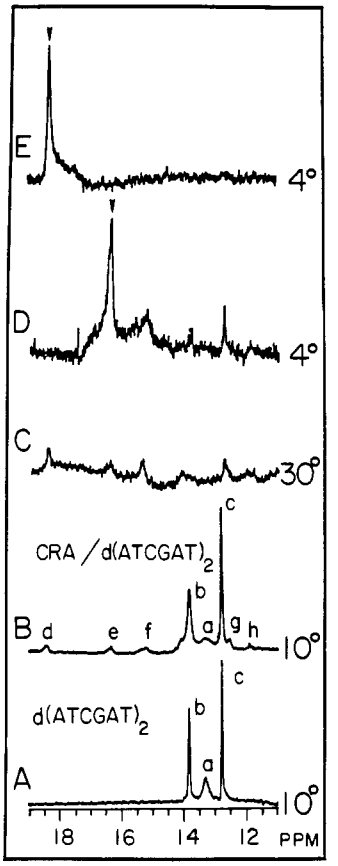

FIGURE 9: Low-field region of 4 mM $d(ATCGAT)_2$ in a borate buffer containing 20 mM Mg^{2+}. Spectra A–C were acquired with a $1\bar{3}3\bar{1}$ pulse sequence. D and E are difference NOE experiments performed in the interleave mode. Spectra A and B were acquired at 10 °C, C at 30 °C, and D and E at 4 °C. The external and internal thymine and the guanine imino protons are labeled as a, b, and c, respectively.

major-groove protons. On the basis of the data discussed below for the complexed octamer CRA–$d(TATGCATA)_2$, where GH8 and TH6 do not overlap, these tentative contacts are assigned to G3H8 and not T2H6. Because of the high density of resonances within this 3.5–4.0 ppm region, alternative assignments cannot be fully dismissed at present.

At the longer mixing times, the 4B and 4OMeB protons have NOE contacts to the 4.27 ppm resonance. This resonance is assigned to drug protons (Cr3′) and DNA protons (C4H3′, T2H4′, or the unassigned C4H5′,H5″). Nevertheless, the drug–drug interaction (Cr3′ to 4B and 4OMeB) is less likely. No second-order NOE contacts are observed from 4B or 4OMeB to the protons closest to Cr3′, i.e., Cr1′, Cr4′, and Cr5′. The alternative assignment of CRA B contacts to the DNA ribose protons is more likely, since both the 4B and 4OMeB resonances contact the 4.27 ppm line. Therefore the 4B and 4OMeB protons could contact the C4H3′, T2H4′, or C4H5′,5″ DNA protons rather than the drug Cr3′ proton. These two B carbohydrate contacts to DNA are consistent with the placement of B in the vicinity of the major groove near G3H8.

Complexes of CRA with Other DNA Sequences

One-Dimensional NMR Studies of CRA–d(ATCGAT)$_2$. Addition of CRA to $d(ATCGAT)_2$ in the ratio of 1 drug: duplex resulted in a broadening of the original imino proton resonances plus the appearance of at least five broad, new resonances (Figure 9, panels A and B). These imino resonances shown in Figure 9B are of relatively low intensity when compared with the $R = 1$ imino proton spectrum of d-

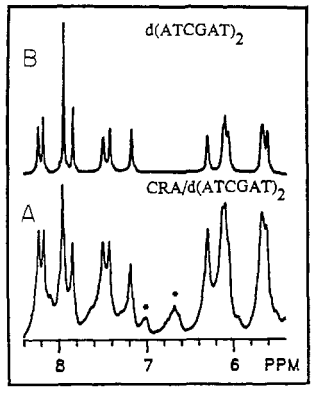

FIGURE 10: Base and deoxyribose proton region of 500-MHz spectra of $d(ATCGAT)_2$ in (A) the presence of CRA ($R = 1$) and (B) the absence of CRA. The asterisks denote the Cr5 and Cr10 protons as described under results. Both spectra were acquired at 15 °C. The samples were prepared in a borate buffer containing 20 mM $MgCl_2$ as described in the text.

$(ATGCAT)_2$ in Figure 2A. Three of these resonances (labeled d–f) are located in the 18–15 ppm region (Figure 9B). The remaining two (labeled g and h) are upfield of G4NH at 12.6 and 11.8 ppm. These spectra are much more complicated than those seen with the $R = 1$ CRA–$d(ATGCAT)_2$ complex (Figure 2A) and are typical of less specific or weak drug binding (Keniry et al., 1987; Marzilli et al., 1986).

Possible assignments of these new resonances can be made by comparisons with the spectra of aggregated CRA in water and of the CRA–$d(ATGCAT)_2$ complex studied above. Peak d at 18 ppm corresponds to the CrOH proton of CRA in water and may indicate the presence of unbound CRA. Irradiation of peak d did not result in an observable NOE to any of the nucleotide imino protons (Figure 9E).

Peak e at 16.4 ppm may be assigned on the basis of comparison with the $d(ATGCAT)_2$ results that show a similar CRA hydroxyl resonance at 16 ppm. Irradiation of e resulted in strong NOE contacts to g and f and weaker NOE contacts to b and h (Figure 9D). Peak f, however, is not assigned. As a CrOH it is shifted extremely far upfield, and as a DNA imino proton resonance it is very far downfield. Peaks f–h may reflect a second, as yet unassigned mode of binding. Raising the temperature from 10 to 30 °C (Figure 9, panels B and C) resulted in exchange broadening of the original imino proton resonances, while the five new resonances (d–h) appear to be less affected.

The aromatic proton region of the $R = 1$ CRA–$d(ATCGAT)_2$ complex, in Figure 10A, is similar to that of the free CG hexamer, in Figure 10B. The only well-resolved drug peaks belong to Cr5 and Cr10 (designated by asterisks in Figure 10A). As with the $d(ATCGAT)_2$ imino proton peaks discussed above, these drug peaks are substantially broader than those observed for the $R = 1$ complex with the GC hexamer (Keniry et al., 1987). They are also in the same resonance positions for unbound chromomycin in water and upfield of the equivalent resonances for other DNA–CRA complexes (Keniry et al., 1987). Hence, these proton NMR data provide evidence that CRA forms a considerably weaker complex with d(ATCGAT) than it forms with d(ATGCAT).

The ^{31}P NMR spectrum of CRA–$d(ATCGAT)_2$ is slightly altered from that of drug-free $d(ATCGAT)_2$. While no new resonances are observed outside of the main band of drug-free resonances (supplementary Figure 3), a small broad resonance is observed on the upfield side of this main band. This broad signal is probably indicative of a small population of complexed $d(ATCGAT)_2$. These results are consistent with the ^1H NMR results above and lend further support to the premise of weak binding.

Imino ^1H NMR Studies of CRA–$d(TATGCATA)_2$. In order to assess whether our results for CRA binding to the GC region of $d(ATGCAT)_2$ have been influenced by the short length of the hexamer, we investigated the CRA complex with the octamer $d(TATGCATA)_2$. The imino proton region of $d(TATGCATA)_2$ alone is similar to that of its hexamer counterpart, $d(ATGCAT)_2$ (supplementary Figure 4). The most upfield resonance is assignable to G4NH, while the neighboring T3NH is assigned to the most downfield resonance. The terminal T1NH is too broad to assign; however, its neighboring T7NH resonance is sharper and partially overlaps with the more protected T3NH resonance.

Addition of chromomycin to a solution containing $d(TATGCATA)_2$ and no added magnesium resulted in a minute amount of drug–DNA binding (<5%). This binding is presumably from residual dications present in the solution. Addition of $MgCl_2$ increases the fraction of chromomycin bound to the octamer (supplementary Figure 4). By a ratio of 0.5 Mg^{2+}:duplex (per drug dimer), the original duplex imino proton signals and the new set of bound signals are present in roughly equal populations. At the ratio of 1 Mg^{2+}:duplex, about 1% of the original signals remain and the titration is essentially complete.

A 200-ms water NOESY spectrum at 15 °C shows most of the same features as those described above for the CRA–$d(ATGCAT)_2$ spectrum. For example, there is a splitting of the labile GNH_2 resonance into two resonances and the appearance of strong cross-strand DNA contacts between G4H1′ and A6H2. Strong drug–DNA contacts from CrOH to A6H1′, C5H1′, and both $G4NH_2$ protons and additional contacts from the E carbohydrate to DNA are observed (E1 to A6H2 and T7H1′, a strong 6MeE to G4H1′ contact, and weaker 6MeE to T3H1′ and A6H2 contacts). Tentatively assigned contacts between the B carbohydrate are also observed (3B and 5B to G4H8). These results with CRA–$d(TATGCATA)_2$ are fully consistent with the binding geometry observed for CRA–$d(ATGCAT)_2$. Hence, the hexamer provides a valid substrate for studying CRA binding.

Imino ^1H NMR Studies of $d(ATAGCTAT)_2$. This octamer allowed us to study the effect of reversing the neighboring AT bases on drug binding. The imino proton region of the octamer at 10 °C consists of three of the four NH resonances assignable to G4 (12.81 ppm), T6 (13.76 ppm), and T2 (13.6 ppm, broad). All assignments were made from 1D NOE studies. By $R = 1$, three new NH signals assigned to the bound form of DNA are observed. Relative to each drug-free resonance, bound G4NH and T6NH are shifted upfield by 0.06 and 0.21 ppm, respectively. Much larger GNH shifts of 0.31 ppm were observed for the hexamer $d(ATGCAT)_2$. The drug CrOH resonance appears as a single peak at 15.85 ppm. Irradiation of CrOH resulted in NOE contacts to both G4NH and T6NH. At $R = 2$, the drug–DNA complex is fully formed, no free DNA resonances are evident, and the bound DNA NH and CrOH resonances are not shifted from the $R = 1$ values. Although these data suggest some differences in binding geometry for this oligonucleotide, the resulting complex possesses C_2 symmetry and is saturated at a ratio of 2 drugs:duplex as described above for $d(ATGCAT)_2$ and $d(TATGCATA)_2$.

Discussion

The stoichiometry and symmetry of the CRA–$d(ATGCAT)_2$ complex, in the presence of excess magnesium, is established by the data shown in Figure 2. At the ratio of 1 CRA:duplex, three new imino resonances corresponding to

bound DNA and the original three imino resonances corresponding to free DNA are both present in approximately equal populations. As the titration proceeds from $R = 1$ to $R = 2$, the free DNA resonances disappear while the three new resonances double in intensity. These results indicate that the stoichiometry of complex formation is 2 CRA molecules:duplex. While it is difficult to prove that, at $R = 1$, the same stoichiometry holds, this appears to be the most likely case. Since six bases contribute to only three bound imino proton resonances at the 2:1 ratio, the drug–DNA complex possesses an apparent 2-fold symmetry about the C_2 axis of d-$(ATGCAT)_2$. These results are a revision of our earlier findings, which suggested a stoichiometry of 1:1 (Keniry et al., 1987). Titration results of CRA binding to the octamer $d(TATGCATA)_2$ are essentially identical with the hexamer results. The inner thymine and guanine imino protons are shifted by similar amounts in both titrations, a 2:1 stoichiometry is observed, and the complex possesses C_2 symmetry. These similarities indicate that the smaller hexamer serves as a reasonable model system for investigating CRA–DNA complexes.

A separate titration was performed to establish the amount of magnesium needed to form the 2:1 drug complex. The titration results described are for the 2:1 complex of CRA bound to $d(TATGCATA)_2$ (supplementary Figure 4). In the absence of magnesium, the addition of CRA to octamer results in no significant binding [the small level of binding (<5%) observed is presumably from residual amounts of dicationic contaminants]. At a stoichiometry of 0.5 Mg^{2+}:duplex, the area of the bound GNH signal is slightly greater than that of the free GNH signal. But by 1.0 Mg^{2+}:duplex (per CRA dimer), the original free GNH signal is essentially gone and a stoichiometry of 1 Mg^{2+}:duplex (per CRA dimer) is apparent.

This stoichiometry of 1 Mg^{2+}:2 drug molecules is in agreement with another recent NMR study (Gao & Patel, 1989a,b) but in disagreement with earlier spectrophotometric studies where a 1 Mg^{2+}:1 CRA stoichiometry was determined (Ward et al., 1965; Hayasaka & Inoue, 1969). Differences in this stoichiometry may be due to the fact that these earlier studies used longer DNA polymers and much lower concentrations of CRA and DNA. At NMR concentrations, Mg^{2+} may facilitate drug binding to DNA by neutralizing the single negative charge on CRA. At a stoichiometry of 1 Mg^{2+}:CRA dimer, the final drug–magnesium complex that binds to DNA would be electrostatically neutral, with Mg^{2+} acting as a bridge between the two drugs.

The CRA protons can be divided into three types: those protons belonging to the carbohydrates (A–E), the chromophore, and the aliphatic side chain. Both the presence and the absence of proton contacts between these three types of CRA protons and the major- or minor-groove protons of d-$(ATGCAT)_2$ are used to assess the structure of the $R = 2$ complex. Strong NOE contacts at 50 ms, from CrOH to $G3NH_2$, C4H1′, and A5H1′, place the hydrophilic edge of chromomycin in the minor groove of $d(ATGCAT)_2$ (Figure 6). The absence of contacts with $C4NH_2$, C4H5, and C4H6 is also consistent with placing the chromophore in the minor groove. A similar binding mode was recently described by Gao and Patel (1989a) with the DNA octamer $d(TTGGCCAA)_2$. Hence, the chromophore lies in the minor groove with CrOH near A5H1′ and C4H1′ of one strand and $G3NH_2$ of the complementary strand. It has been proposed that hydrogen bonding between GNH_2 and a CRA hydroxyl or carbonyl group may be responsible for the selective binding of CRA to the guanine regions of DNA (Brickenshtein et al., 1985). Both the closeness of CrOH to $G3NH_2$ and the hindered rotation about the G3 amino carbon–nitrogen bond are consistent with this hydrogen-bonding model. The chromophore carbonyl nearby (C1=O) or an ionized hydroxyl group (e.g., $C9O^-$ or $C8O^-$) is available for hydrogen bonding with the nearby guanine amino protons.

In addition to CrOH, the CRA E carbohydrate also shows prominent NOE contacts to the DNA minor groove (Figure 7). Contacts between 1E/A5H2, 1E/T6H1′, and 4E/T2H1′ are observed at all three NOE mixing times. These NOE contacts involve drug proton resonances in a less crowded spectral region and are consistent with a parallel study involving the chromomycin analogue mithramycin (unpublished results). Therefore, both the E carbohydrate and the hydrophilic edge are positioned in the minor groove of d-$(ATGCAT)_2$. T6H1′ is spatially located near A5H2 on the same strand and can easily share a mutual contact with 1E, while the 4E proton can be positioned near T2H1′ on the opposite strand. By positioning E in this manner and directing the chromophore toward the C_2 axis of symmetry, D is positioned near the sugar–phosphate backbone.

With the exception of the contacts between the chromomycin E and DNA protons, it is remarkable that so few additional nonlabile drug-to-DNA proton contacts are observed. For example, the adjacent CD and AB carbohydrates show no 50-ms NOESY contacts with DNA. This absence of observable contacts suggests that these carbohydrates are out of the groove, placed along or around the sugar–phosphate backbone. If chromomycin is predominantly located outside the minor groove, then the nonlabile contacts among the H5′, H5″, and H4′ deoxyribose protons with the drug protons are expected. Unfortunately, the H5′ and H5″ protons are not easily assigned and the H4′ proton resonances appear in a crowded region of the proton spectrum.

The results presented above on the CRA–$d(ATGCAT)_2$ complex at $R = 2$ are in agreement with our previous data on the $R = 1$ complex in terms of prominent drug proton contacts to the major-groove protons of DNA at the longer mixing times (200 and 400 ms). For example, potential drug–DNA contacts from G3H8 to 3B and 5B protons place the B carbohydrate around the sugar–phosphate backbone, near the major groove. This orientation is consistent with the chromophore contacts in the minor groove. Similar contacts were also observed with the octamer $d(ACCCGGGT)_2$ (unpublished data). However, from these B carbohydrate contacts and weak contacts between the chromophore methyl and the major groove, we originally concluded that the entire drug molecule was in the major groove of DNA (Keniry et al., 1987). More proton assignments were made in the present study including those of the E carbohydrate and some of the amino protons of DNA. The result is that a large portion of the drug is closely associated with the minor-groove side of DNA and not the major-groove side as previously concluded.

The tentatively assigned acetoxy resonances of E and A also have NOE contacts with the major-groove protons T2Me and C4H6, respectively. Clearly the assignment of these resonances and the placement of the A and B carbohydrates require further study, but their role in the guanine base selectivity of chromomycin may not be as important as that of the chromophore hydroxyl, which is more intimately involved within the minor groove of DNA. Recent NMR studies by Kam (1988) have shown that a chromomycin analogue missing the B carbohydrate moiety can still bind to $d(ATGCAT)_2$ with a slightly lower binding affinity than CRA itself. This is in

agreement with earlier polymerase studies (Behr et al., 1969; Kaziro & Kamiyama, 1967).

When drug–drug proton contacts between the carbohydrates, the chromophore, and the aliphatic side chain are evaluated by using molecular models, an approximate picture of the chromomycin conformation begins to emerge. The presence of only one contact from the A carbohydrate to the chromophore positions the 1A proton near Cr5 on the hydrophobic edge of the chromophore and implicitly away from the nearby Cr7 methyl protons. NOE contacts between A and B carbohydrates are sufficient to determine that B is positioned away from the hydrophobic edge. This is supported by the absence of B carbohydrate contacts to the protons along this edge (Cr5, Cr10, Cr4e, and Cr4a) and is consistent with weak B contacts to G3H8.

Like the A carbohydrate, the C carbohydrate can be positioned with respect to the chromophore. Contacts from 1C and 5C to Cr2 imply that the C1–O–C5 portion of C points toward the aliphatic side chain. This is further supported by the 50-ms contact between 5C and Cr1′OMe of the aliphatic side chain. Placement of D with respect to C is much more difficult. Only one contact is observed between 5D and the 2eC resonance at 2.27 ppm. Since this resonance is shared by 2eC and three other drug protons, this D to C contact is tentative. There are no additional C to D or C to E contacts to support this assignment.

Several D to E contacts are self-consistent and indicate a conformation where the 3MeE is placed over the D ring toward the 4D proton. A strong 5D contact to Cr5 of the chromophore can be interpreted in one of two ways. As an intramolecular contact, the CDE chain is partially folded over the hydrophobic edge of its own chromophore. As an intermolecular contact, the CDE chain overlaps with the other chromophore. In agreement with the results of Gao and Patel (1989a), we observe a strong coupling between the chromophore Cr2 and Cr3 protons. This places these protons diaxial to each other and effectively moves the CDE chain away from its own chromophore ring. Hence, these data imply that the CDE chain is directed away from its own ring while overlapping its D ring with the neighboring chromophore ring.

Contacts between the aliphatic side chain and the chromophore are minimal at the 50-ms mixing time studied. Cr1′ shows contacts to the Cr2 and Cr3,4a protons. As discussed previously, cross-peaks between the aliphatic chain protons and the Cr10 and Cr5 protons are observed at the longer mixing times and are indicative of long-range contacts (Keniry et al., 1987). These contacts place the aliphatic side chain in the vicinity of the hydrophobic edge but not necessarily within 4 Å of the Cr10 and Cr5 protons.

Some degree of asymmetry is indicated by unassigned NOESY cross-peaks that correspond to CRA protons in the upfield region (<4 ppm). Since the drug is in slow exchange with $d(ATGCAT)_2$ on the NMR time scale, it can be assumed that these cross-peaks represent distinct variations in portions of the carbohydrate or aliphatic side chains.

On the basis of the proton NOESY data for the 2:1 complex, the hexamer $d(ATGCAT)_2$ appears to lose some of its B-DNA character while obtaining some A-DNA characteristics. The direction and degree of these changes can be evaluated by comparing changes in the 50-ms NOE intensities between the free and drug-bound hexamer with those calculated from computer-generated models of $d(ATGCAT)_2$ in the Arnott A-DNA and B-DNA conformations. Some of these results are shown in Figure 11. Clearly the hexamer duplex has been altered by CRA but not to the degree of

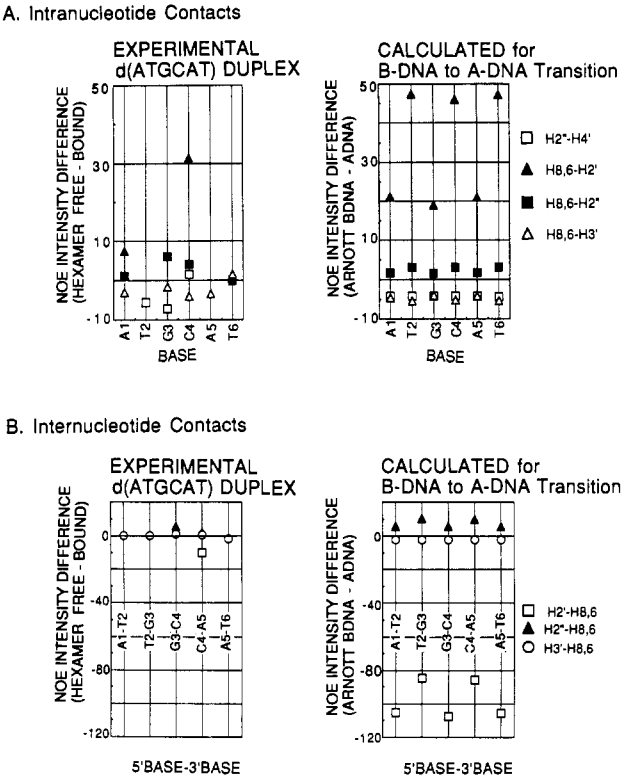

FIGURE 11: Conformational differences of $d(ATGCAT)_2$ between the CRA-free and CRA-bound state compared with the computer-generated models of this hexamer in the Arnott B- and A-DNA forms (Borgias & James, 1988). Differences in the NOE intensities are plotted for each nucleotide. Experimental intensity differences (left side) are compared with computer-generated differences (right side). In the case of chemical shift overlap for the experimental data, the difference was not included.

forming the Arnott A-DNA structure. However, elements of the A-DNA structure are inferred by the direction of the intensity changes. For example, addition of CRA brings about an increase in the T2 and G3 intranucleotide intensities between H2″ and H4′ and an increase in the intensities between H8, H6 and H3′ for A1, T2, G3, C4, and A5 (Figure 11A and Table III). The magnitude of these latter intensity increases is supported by a corresponding decrease in the H8,H6/H2″ intensities for G3 and C4 and in the C4 H6/H2′ intensity. These intensity changes are consistent with a more C3′ endo sugar pucker, as expected for A-DNA.

In the case of the internucleotide contacts, these intensity changes are not exemplary of a B-DNA to A-DNA transition (Figure 11B). The magnitude of the intensity changes is not as large as those calculated for the A-DNA contacts between C4H2′ and A5H8 and between H2″ and H8,H6 of G3 to C4 and C4 to A5. Furthermore, the magnitude and direction of the H3′ to H8,H6 intensity changes for G3 to C4 and for C4 to A5 do not correspond to the predicted values for A-DNA. Nevertheless, the cross-strand contact between G3H1′ and A5H2 does increase upon CRA binding as expected for an A-like DNA structure, with its typically wider and shallower groove. Hence the conformation of the CRA-bound duplex $d(ATGCAT)_2$ is altered to various degrees along the helix, containing some properties of both the B-DNA and A-DNA helices. A widened minor groove was also described for two closely placed actinomycin D molecules bound to d-(ATGCGCAT) by Scott et al. (1988) as well as by Gao and Patel (1989a) in their study with the CRA–d(TTGGCCAA) complex.

In general, the structural features of a CRA complex with DNA as described by Gao and Patel for d(TTGGCCAA)

were very similar to our own observations for d(ATGCAT): NOE contacts (1) orient the AB chain away from the chromophore ring, (2) orient the D carbohydrate above the chromophore ring of the neighboring drug molecule, (3) orient the hydrophilic edge of the chromophore in the minor groove near GNH_2 and CH1′, and (4) orient the E carbohydrate in the minor groove. On the basis of these four features, it appears that the orientation of CRA does not vary greatly between these two sequences. However, the placement of adenine in our sequence does demonstrate a tight association between the E carbohydrate and the minor groove by virtue of several strong 50-ms NOE contacts, including the contact between 1E and the minor-groove proton A5H2. Furthermore, weak B carbohydrate contacts with the major-groove protons suggest that the AB chain extends around the sugar–phosphate backbone with the B ring pointed into the major groove as previously described in our earlier paper (Keniry et al., 1987). Similar B carbohydrate contacts are not described in the paper of Gao and Patel (1989a,b), and this may suggest subtle differences in the way CRA binds to d(TTGGCCAA) and d(ATGCAT). However, Gao and Patel (1989a) do report a weak NOE contact between the chromomycin chromophore C7 methyl group and the C5H6 proton in the major groove, which we also described earlier (Keniry et al., 1987).

Three of the four sequences studied here and the sequences of Gao and Patel (1989a,b), d(TTG*GC*CAA) and d(AAG*GC*CTT), contain two central GC bases and exhibit strong selective binding at this central site to form C_2 symmetric complexes with the CRA dimer. In contrast, the CG-containing sequence d(AT*CG*AT) exhibits weak binding at its central site. Preliminary results obtained with d(ACC*CGG*GT) show strong binding. However, these results suggest that the complex formed is not a single C_2 symmetric complex (unpublished results). On the basis of these comparisons, the CRA dimer appears to have a higher selectivity for the centrally located GC sequence than for the CG sequence. Characteristic differences in the size and shape of the minor groove between these two sequences plus the orientation of the electrostatically positive GNH_2 protons probably affect the stability of the drug–DNA complex.

Conclusion

Our present study shows that chromomycin binds to d(ATGCAT)$_2$ by placing its hydrophilic edge and E carbohydrate in the minor groove of the duplex. This is similar to the results found by Gao and Patel with the sequence d(TTGGCCAA) (Gao & Patel, 1989a). Drug-induced conformational changes in the DNA helix possess some characteristics of both B-DNA and A-DNA, where the minor groove is wider and more shallow. Hence, each DNA duplex is capable of accommodating two of these bulky chromomycin molecules to form an effectively C_2 symmetric drug–DNA complex. No evidence was found that would place other portions of the drug in the minor groove. The implication of these observations, together with those of earlier studies (Behr et al., 1969; Kaziro & Kamiyama, 1967), is that while the AB and CDE chains play a role in the binding affinity of chromomycin, the chromophore hydrophilic edge is in a position to facilitate hydrogen bonding with the guanine amino protons. The presence of guanine alone, however, is not sufficient for strong selective binding, as evidenced by our study with the hexamer d(ATCGAT)$_2$. Thus chromomycin exhibits a strong sequence selectivity in addition to base composition specificity. Further studies including energy-minimized models of chromomycin dimer binding to d(ATGCAT)$_2$ in comparison to d(ATCGAT)$_2$ are presently underway in our laboratory.

Acknowledgments

We thank Dr. B. Borgias and Prof. T. L. James for making CORMA available and Dr. C. Levenson, Cetus Corp., for the generous gift of d(ATAGCTAT)$_2$ octamer.

Supplementary Material Available

Four figures showing ^{31}P NMR spectra of 1:1 and 2:1 CRA:d(ATGCAT)$_2$ complexes, 50-ms COSY and NOESY spectra of drug-free d(ATGCAT)$_2$, ^{31}P NMR spectra of d(ATCGAT)$_2$ alone and in a 1:1 complex with CRA, and Mg^{2+} titration of a 2:1 mixture of CRA and d(TATGCATA)$_2$ (4 pages). Ordering information is given on any current masthead page.

References

Arnott, S., & Hukins, D. W. L. (1972) *Biochem. Biophys. Res. Commun. 47*, 1504–1510.
Aue, W. P., Barthoholdi, E., & Ernst, R. R. (1976) *J. Chem. Phys. 64*, 2229–2246.
Bax, A., & Davis, D. G. (1985) *J. Magn. Reson. 65*, 355–360.
Bax, A., & Lerner, L. (1988) *J. Magn. Reson. 79*, 429–438.
Behr, W., & Hartmann, G. (1965) *Biochem. Z. 343*, 519–527.
Behr, W., Honikel, K., & Hartmann, G. (1969) *Eur. J. Biochem. 9*, 82–92.
Berlin, Y., Espinov, S., Kolosov, M., & Shemyakin, M. (1966) *Tetrahedron Lett.*, 1643–1647.
Berman, E., & Shafer, R. H. (1983) *Biopolymers 22*, 2163–2167.
Berman, E., Brown, S. C., James, T. L., & Shafer, R. H. (1985) *Biochemistry 24*, 6887–6893.
Bodenhausen, G., Vold, R. L., & Vold, R. R. (1980) *J. Magn. Reson. 37*, 93–106.
Borgias, B. A., & James, T. L. (1988) *J. Magn. Reson. 79*, 493–512.
Brikenshtein, V. Kh., Pitina, L. R., Barenboim, G. M., & Gurskii, G. V. (1983) *Mol. Biol. (Moscow) 18*, 1606–1616.
Chou, S. H., Hare, D. R., Wemmer, D. E., & Reid, B. R. (1983) *Biochemistry 22*, 3037–3041.
Cobreros, G., Lopez Zumel, M. C., & Usobiaga, P. (1982) *Radiat. Res. 92*, 255–267.
Dagleish, D. G., Fey, G., & Kersten, W. (1974) *Biopolymers 13*, 1757–1766.
Davis, D. G., & Bax, A. (1985) *J. Magn. Reson. 64*, 533–535.
Fox, K. R., & Howarth, N. R. (1985) *Nucleic Acids Res. 13*, 8695–8714.
Fox, K. R., & Waring, M. J. (1986) *Nucleic Acids Res. 14*, 2001–2014.
Gao, X., & Patel, D. J. (1989a) *Biochemistry 28*, 751–762.
Gao, X., & Patel, D. J. (1989b) *Q. Rev. Biophys. 22*, 93–138.
Gause, G. F. (1965) *Adv. Chemother. 2*, 179–194.
Hartmann, G., Behr, W., Beissner, K.-A., Honikel, K., & Sippel, A. (1968) *Angew. Chem., Int. Ed. Engl. 7*, 693–701.
Hartmann, S. R., & Hahn, E. L. (1962) *Phys. Rev. 128*, 2042–2053.
Hayasaka, T., & Inoue, Y. (1969) *Biochemistry 8*, 2342–2347.
Hore, P. J. (1983) *J. Magn. Reson. 55*, 283–300.
Horwitz, K. B., & McGuire, W. L. (1978) *J. Biol. Chem. 253*, 6319–6322.
Jamin, N., James, T. L., & Zon, G. (1985) *Eur. J. Biochem. 152*, 157–166.
Kam, M. (1988) M.S. Thesis, The Weizmann Institute of Science, Rehovot, Israel.
Kam, M., Shafer, R. H., & Berman, E. (1988) *Biochemistry 27*, 3581–3588.
Kaziro, Y., & Kamiyama, M. (1967) *J. Biochem. (Tokyo) 62*, 424–429.

Keniry, M. A., Brown, S. C., Berman, E., & Shafer, R. H. (1987) *Biochemistry 26*, 1058-1067.
Kersten, H., & Kersten, W. (1974) *Mol. Biol., Biochem. Biophys. 18*, 86-89.
Kersten, W., & Kersten, H. (1965) *Biochem. Z. 341*, 174-183.
Kersten, W., Kersten, H., & Szybalski, W. (1966) *Biochemistry 5*, 236-244.
Kersten, W., Kersten, H., Steiner, F., & Emmerich, B. (1967) *Hoppe-Seyler's Z. Physiol. Chem. 348*, 1415-1423.
Marion, D., & Wuthrich, K. (1983) *Biochem. Biophys. Res. Commun. 113*, 967-974.
Marion, D., & Lancelot, G. (1984) *Biochem. Biophys. Res. Commun. 124*, 774-783.
Marzilli, G., Banville, D. L., Zon, G., & Wilson, W. D. (1986) *J. Am. Chem. Soc. 108*, 4188-4192.
McConnell, B., & Politowski, D. (1984) *Biophys. Chem. 20*, 135-148.
Miyamoto, M., Kawamatsu, Y., Kawashima, K., Shinohara, M., & Nakanishi, K. (1966) *Tetrahedron Lett.*, 545-552.
Nayak, R., Sirsi, M., & Podder, S. K. (1973) *FEBS Lett. 30*, 157-162.
Neuhaus, D., Wagner, G., Vasak, M., Kagi, J. H. R., & Wuthrich, K. (1985) *Eur. J. Biochem. 151*, 257-273.
Patel, D. J. (1987) Communication at the International Congress on Nucleic Acid Interactions, Padova, Italy.
Redfield, A. G., & Kunz, S. D. (1975) *J. Magn. Reson. 19*, 250-254.
Remers, W. A. (1979) in *The Chemistry of Antitumor Antibiotics*, Wiley, New York.
Scott, E. V., Zon, G., Marzilli, L. G., & Wilson, W. D. (1988) *Biochemistry 27*, 7940-7951.
Shaka, A. J., & Keeler, J. (1987) *Prog. Nucl. Magn. Reson. Spectrosc. 19*, 47-129.
Slavek, M., & Carter, S. K. (1975) *Adv. Pharmacol. Chemother. 12*, 1-30.
States, D. J., Haberkorn, R. A., & Ruben, D. J. (1982) *J. Magn. Reson. 48*, 286-292.
Thiem, J., & Meyer, B. (1979) *J. Chem. Soc., Perkin Trans. 2*, 1331-1336.
Thiem, J., & Meyer, B. (1981) *Tetrahedron 37*, 551-558.
Ulrich, E. L., John, E. M. M., Gough, G. R., Brunden, M. J., Gilham, P. T., Westler, W. M., & Markley, J. L. (1983) *Biochemistry 22*, 4362-4365.
Van Dyke, M. W., & Dervan, P. B. (1983) *Biochemistry 22*, 2372-2377.
Wakisaka, G., Uchino, H., Nakamura, T. Sotobayashi, M., Shirakaw, S., Adachi, A., & Sakurai, M. (1963) *Nature (London) 198*, 385-386.
Ward, D., Reich, E., & Goldberg, I. (1965) *Science (Washington, D.C.) 149*, 1259-1263.
Waring, M. (1970) *J. Mol. Biol. 54*, 247-279.
Wuthrich, R. (1986) in *NMR of Proteins and Nucleic Acids*, Wiley-Interscience, New York.

Minimum Secondary Structure Requirements for Catalytic Activity of a Self-Splicing Group I Intron†

Amber A. Beaudry and Gerald F. Joyce*
Department of Chemistry and Department of Molecular Biology, Research Institute of Scripps Clinic, La Jolla, California 92037

Received January 19, 1990; Revised Manuscript Received April 4, 1990

ABSTRACT: We have completed a comprehensive deletion analysis of the *Tetrahymena* ribozyme in order to define the minimum secondary structure requirements for phosphoester transfer activity of a self-splicing group I intron. A total of 299 nucleotides were removed in a piecewise fashion, leaving a catalytic core of 114 nucleotides that form 7 base-paired structural elements. Among the various deletion mutants are a 300-nucleotide single-deletion mutant and a 281-nucleotide double-deletion mutant whose activity exceeds that of the wild type when tested under physiologic conditions. Consideration of those structural elements that are essential for catalytic activity leads to a simplified secondary structure model of the catalytic core of a group I intron.

The *Tetrahymena* ribozyme catalyzes sequence-specific phosphoester transfer reactions involving nucleic acid substrates (Zaug & Cech, 1985; Kay & Inoue, 1987). The specificity of this reaction is determined by binding of an oligopyrimidine substrate to a sequence of purines located near the 5′ end of the enzyme (Been & Cech, 1986; Waring et al., 1986) and by binding of a guanosine substrate to a G·C base pair located within the central portion of the molecule (Michel et al., 1989). The detailed chemistry of the reaction is not known, but is thought to proceed by an S_N2 (P) mechanism involving inversion of configuration at phosphorus (McSwiggen & Cech, 1989; Rajagopal et al., 1989). A 3′-terminal guanosine residue, for example, can act as a nucleophile to attack a phosphodiester bond following a sequence of pyrimidines. The products of the reaction are guanosine joined to whatever residues lie downstream from the target phosphodiester and oligopyrimidine with a free 2′- and 3′-hydroxyl. We have used this reaction as an assay to study the structural basis of catalytic activity of the *Tetrahymena* ribozyme and to develop variant forms of the molecule that retain catalytic activity.

The *Tetrahymena* ribozyme is categorized as a group I intron based on the presence of several short highly conserved sequence elements that result in characteristic features of local secondary structure (Davies et al., 1982; Michel et al., 1982;

† Supported by the National Aeronautics and Space Administration (NAGW-1671).
* Author to whom correspondence should be addressed.

0006-2960/90/0429-6534$02.50/0